ICSV13 - Vienna
The Thirteenth International Congress on Sound and Vibration
Vienna, Austria, July 2-6, 2006

ACTIVE NOISE CONTROL WITH MOVING ERROR MICROPHONE: PRELIMINARY RESULTS

Małgorzata I. Michalczyk, and Krzysztof Czyż*

Silesian University of Technology, Institute of Automatic Control
Akademicka 16
44-100 Gliwice, Poland
malgorzata.michalczyk@polsl.pl

Abstract

The paper concerns the single-channel active noise control system creating 3-dimensional zone of quiet in enclosure. Due to the use of adaptive control algorithm the created zone of quiet can adaptively track the movement of the error microphone. The movement of the zone of quiet depends on the velocity of the error microphone and the adaptation parameter. All observations are made on the basis of the real-world active noise control system and are illustrated by the results of experiments performed on the special laboratory stand.

INTRODUCTION

The electro-acoustic plants controlled by active noise control (ANC) systems in enclosures are usually time-varying. Some of variations are caused by changes of air temperature and humidity or movements of objects or persons in the enclosure. To deal with these variations adaptation is applied to the control algorithms, what is widely described in the literature [2,3]. However, the type of the ANC system discussed in the paper is designed to assure low noise level around the moving user. In this case, the time variations of the electro-acoustic plant are fast, as the person equipped with the error microphone can move quickly. The use of adaptive ANC algorithms for tracking of fast variations of error microphone position has been hardly analysed so far.

Adaptive control algorithms are used for initial calculation of controller coefficients and to deal with slow changes of an electro-acoustic plant. For such tasks the adaptation is set to be slow. When the ANC system is tracking moving error microphone adaptive control algorithm has to be parameterised in a different way – the adaptation is set to be fast enough to track the movements of the error microphone. The paper presents the results of preliminary real-world experiments concerning the behaviour of the ANC system with moving error microphone.

ACTIVE NOISE CONTROL SYSTEM

The ANC system presented in this paper is used to create 3-dimensional zones of quiet in enclosure of cubature of 70 m^3 (Fig. 1). It is the one-channel adaptive system of feedforward structure with reference microphone (M_x in Fig. 1). The zone of quiet is created around the error microphone M_e (Figs 1-2) that picks up the error signal. Two channels of the electro-acoustic plant can be defined: a secondary path, including electronic instrumentation and acoustic part of the enclosure between the control loudspeaker and the error microphone, and the acoustic feedback path. The error microphone M_e can move - it implies that the secondary path changes in time.

Figure 1 – ANC system for creation of 3D zones of quiet in enclosure.

The adaptive controller is applied, employing FX-LMS (Filtered-X Least Mean Squares) algorithm [2,3,5] with neutralisation of acoustic feedback [2,3,5]. The identification of electro-acoustic plant models necessary for parameterisation of the control algorithm is performed before the activation of the ANC system [5] with the error microphone located in position M_1 (Fig. 2) in the distance of 0.5 m from the control loudspeaker. The controller FIR filter order has been N = 500 and FX-LMS algorithm adaptation parameter μ has been chosen experimentally [4]. The control algorithm has been implemented in TMS320C31 Texas Instruments DSP on dSPACE 1102 Board. The sampling frequency was equal 500 Hz.

In order to evaluate the influence of the movement of the error microphone on the ANC system performance a special laboratory stand was build (Fig. 2). It enables to move the error microphone round the circle trajectory with constant or variable rotational speed. Four observation microphones – M_1, M_2, M_3 and M_4 – are located around the circle (Fig. 2), about 1 cm over the trajectory of the error microphone. The additional observation microphone M_0 is located 20 cm over the centre of the circle.

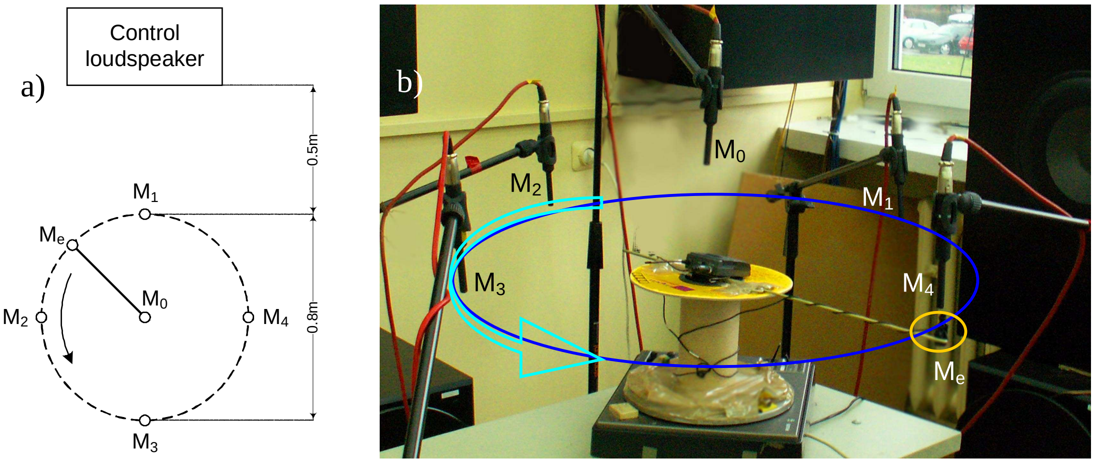

Figure 2 – The laboratory stand enabling the movement of the error microphone and the observation microphones positions: a) scheme and b) photo(error microphone trajectory denoted with blue circle).

The observation microphones have been used to pick up the signals, that along with the error microphone signal have been sampled with frequency of 10 kHz and recorded using dSPACE 1104 Board. Using the recorded data the disturbance attenuation in all microphones was calculated.

The rotational speed can range from about 0.2 to 1.4 rotations per second. In the experiments presented in this paper the diameter of the circle has been set on 0.8 m, thus the linear velocity of the error microphone has ranged from 1 to 7 m/s.

ELECTRO-ACOUSTIC PLANT NONSTATIONARITIES

The electro-acoustic plant controlled by the ANC system includes electronic elements and an acoustic space. The acoustic space can change very significantly, especially if it is the inside of enclosure. Every change of the enclosure spatial configuration causes an inevitable large change of electro-acoustic plant dynamic properties. The electro-acoustic plant nonstationarities can be split into three groups [4,5]:

a) weak nonstationarities, caused by changes of air temperature and humidity, mains supply frequency fluctuations, etc. They do not introduce significant changes of electro-acoustic plant dynamics and therefore do not influence ANC systems performance.

b) strong nonstationarities, caused by externally introduced changes to the ANC system environment: any movements of persons in the enclosure, location changes of furniture, opening or closing of door or windows. Transducers (microphones and control loudspeakers) locations are assumed to be fixed. Door opening and person movement inside the enclosure [4], which cause strong nonstationarities of the acoustic feedback path can also serve as an example. The applied control algorithm is robust on such changes of the secondary path [4].

c) severe nonstationarities, caused by movements of the error microphone in the enclosure. Such movements cause huge changes in the secondary path dynamics, especially changes of the phase. The increase of the phase estimation error, if exceeds $\pm\pi/2$, results in divergence of the adaptive control algorithm [2,3]. The change of the magnitude of the secondary path may also result in control algorithm divergence, if the adaptation parameter is too large.

If the spatial range of severe nonstationarities is small, i.e. generated by small (comparison with the disturbance wavelength) dislocations of the error microphone it was shown that that kind of severe nonstationarities can be dealt with the use of standard adaptive control algorithm. The preliminary experiments that gave promising results were reported in [1] and are also continued in this paper. Severe nonstationarities of a wide spatial range can be generated by large dislocations of the error microphone or by significant changes of the secondary path dynamics. In such case the electro-acoustic plant models should be additionally identified *on-line* [2,3,4].

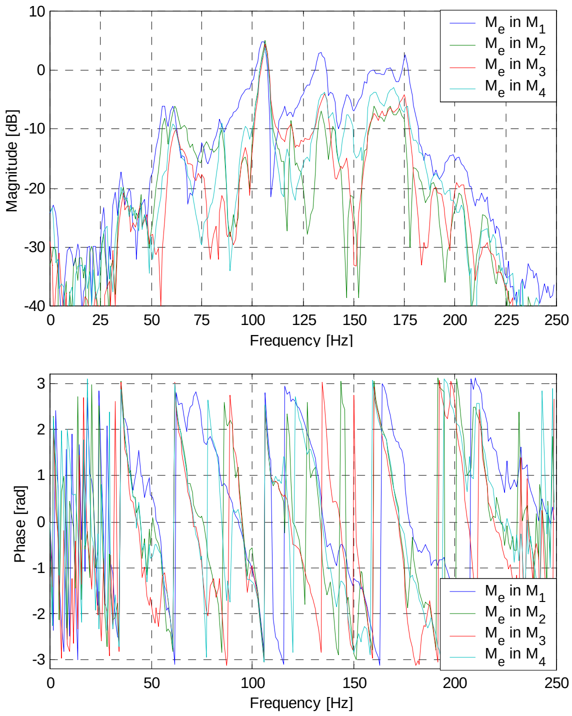

Figure 3 – Frequency response of the secondary path for the error microphone M_e located in M_1, M_2, M_3 and M_4 observation positions.

The frequency responses of the secondary path for four locations of the error microphone are shown in Fig. 3. It can be seen that for some frequencies there are large variations in magnitude as well as in phase. It is imposed by complicated dynamics of the reverberant enclosure. However, for some frequencies the variations are small, e.g. a few decibels of a difference in magnitude and negligible variations in phase for frequency 105 Hz. Thus, for preliminary experiments the periodic disturbance of frequency 105 Hz (pure tone) was chosen.

RESULTS OF REAL-WORLD EXPERIMENTS

Large number of real-world experiments have been conducted to observe the behaviour of the ANC system with moving error microphone. The linear velocity of the error microphone has been set to values: v = 1, 2, 3, 4 and 7 m/s. Adaptation parameter values has been set to values $\mu = 10^{-6}$, 10^{-5}, $5*10^{-5}$, 10^{-4} and $1.2*10^{-4}$.

The disturbance attenuation has been calculated in two ways. For stationary conditions (error microphone velocity equal 0 m/s) the disturbance attenuation has been calculated according to formula:

$$J = -10\log_{10}\left(\frac{\hat{\sigma}_e^2}{\hat{\sigma}_d^2}\right) \tag{1}$$

where $\hat{\sigma}_e^2$ and $\hat{\sigma}_d^2$ are the estimates of the variance of the error and the disturbance signal. For nonstationary conditions (moving error microphone) the disturbance attenuation was calculated in the following way:

$$J(i) = J(iT) = -10\log_{10}\left(\frac{\hat{\sigma}'^2_e(i)}{\hat{\sigma}'^2_d(i)}\right) \tag{2}$$

where the estimate of the variance $\hat{\sigma}'^2_e(i)$ of the error signal $e(i)$ was calculated for the ANC system activated in two steps. The first was the calculation of the error signal power with exponential smoothing $\hat{\sigma}_e^2(i) = \alpha\hat{\sigma}_e^2(i-1) + (1-\alpha)e^2(i)$ with experimentally chosen smoothing factor $\alpha = 0.997$. The second step was the additional smoothing of the obtained error signal power $\hat{\sigma}_e^2(i)$ estimate using moving average $\hat{\sigma}'^2_e(i) = MA\{\hat{\sigma}_e^2(i)\}$ with the window length $N_{MA} = 48$. Disturbance signal $d(i)$ power estimate $\hat{\sigma}'^2_d(i)$ was calculated in the same way. All measurements have been taken after the initial adaptation stage.

Stationary conditions

In the stationary conditions the disturbance of the frequency 105 Hz is attenuated to the background noise level, $J = 28 \div 33$ dB dependently on the location of the error microphone. If the error microphone is located in the position M_1 the attenuation J in the observation microphones is correspondingly 15 dB in M_0, 28.5 dB in M_1, 6 dB in M_2, 12 dB in M_3 and 5.5 dB in M_4.

Moving zone of quiet

Figures 4 and 5 show the movement of zone of quiet. In Fig. 4 the attenuation $J(i)$ in the observation microphone M_1 is shown as a function of time, corresponding to the error microphone position for the linear velocity v = 1 m/s. Three attenuation $J(i)$

curves have been obtained with adaptation parameter values $\mu = 10^{-6}$, 10^{-5} and 10^{-4}. It can be noticed that almost constant attenuation is observed for the lowest adaptation parameter value – $J(i)$ only slightly oscillates around 13 dB level. For larger μ value the ANC system starts to track the error microphone – attenuation $J(i)$ changes from 5 to over 15 dB. However, maximum attenuation $J(i)$ is obtained about 0.65 s after the error microphone goes through the position M_1. It means that the zone of quiet tracks the error microphone, but is delayed. For the highest value of the adaptation parameter $\mu = 10^{-4}$ attenuation changes from 2 to 33 dB. Now, the highest attenuation is obtained almost exactly in the moment the error microphone goes through the observation position. It means, that the zone of quiet moves with the error microphone, surrounding it.

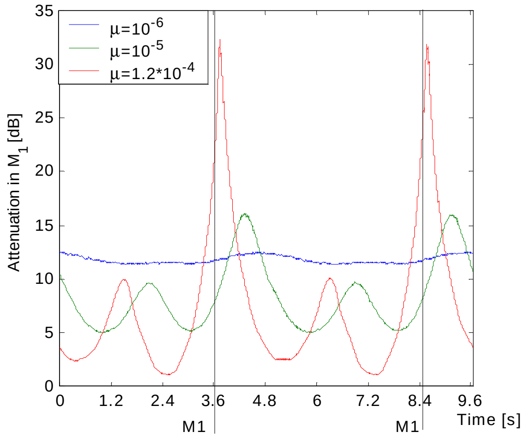

Figure 4 – Attenuation J(i) obtained in observation microphone M_1 for the v = 1 m/s and for different values of μ.

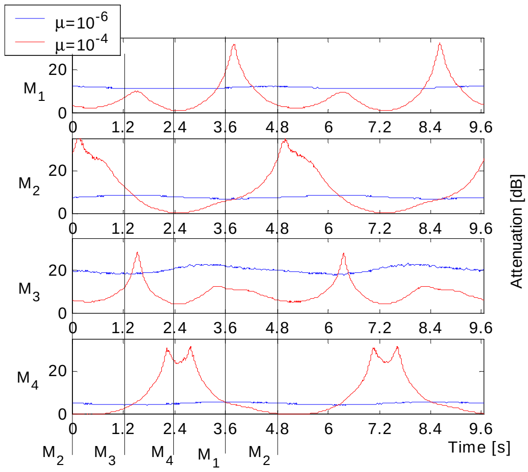

Figure 5 – Attenuation J(i) obtained in 4 observation microphones for v = 1 m/s and for different values of μ.

The arrangement of the time plots of the $J(i)$ obtained in four observation microphones for the error microphone velocity v = 1 m/s and adaptation parameter $\mu = 10^{-4}$ (and $\mu = 10^{-6}$ for comparison) shows how the zone of quiet moves around the circle (Fig. 5). The position of the error microphone in relation to the observation microphones is denoted by the vertical lines. The highest attenuation is obtained for larger adaptation parameter value at the moment the error microphone goes through the observation position.

It is worth to mention that for some time intervals the attenuation in the observation microphone is smaller for larger adaptation parameter values than for no (or very slow) adaptation. It shows that for larger adaptation parameter values the zone of quiet is smaller, however, the higher attenuation is obtained in its centre.

Influence of the adaptation parameter

The larger value of the adaptation parameter μ, the higher is the speed of convergence of the FX-LMS algorithm. Consequently, by increasing the adaptation parameter value for the constant linear velocity of the error microphone the higher attenuation is obtained. This is illustrated by the attenuation $J(i)$ curves in Fig. 6, in which attenuation for the slow movement of the error microphone (v = 1 m/s) and for different adaptation parameter values are shown. Obtained attenuation varies from 5 ÷ 20 dB for the lowest μ value to 22 ÷ 34 dB for the largest μ value. The attenuation fluctuates even for the $\mu = 1.2*10^{-4}$ because of the dynamical properties of the electro-acoustic plant.

The influence of the adaptation parameter is also illustrated in Fig. 7. The Maximum value of the obtained attenuation $J(i)$ is shown as a function of the error microphone velocity and the adaptation parameter value. Again, the larger μ value, the higher is the attenuation.

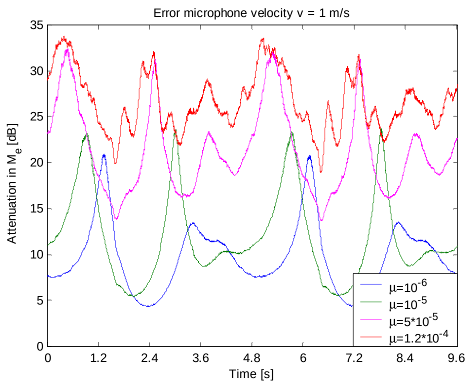

Figure 6 – Attenuation J(i) obtained in the error microphone for v = 1 m/s and for different values of μ.

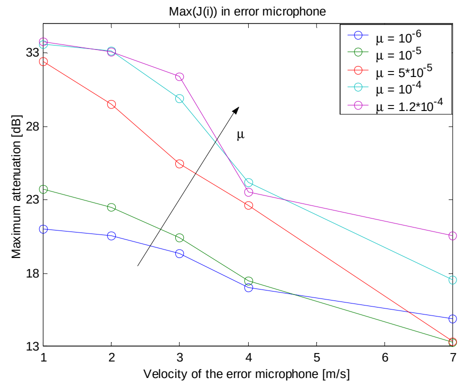

Figure 7 – Maximum attenuation J(i) obtained in the error microphone for different values of v and of μ.

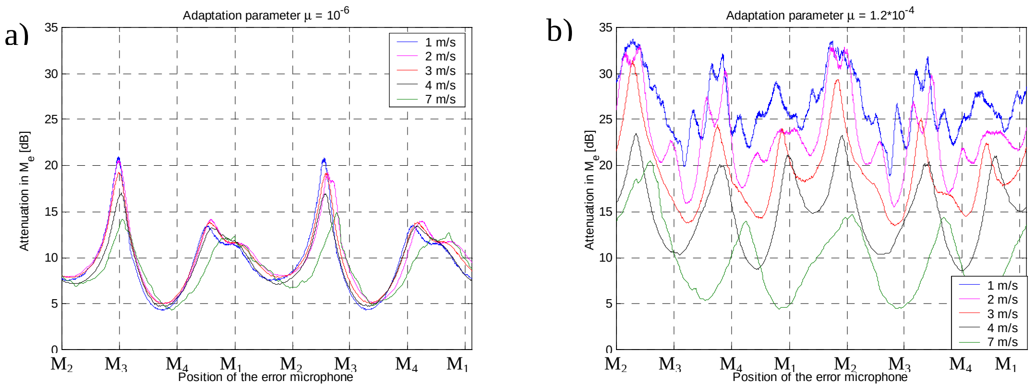

Figure 8 – Attenuation J(i) in error microphone for different v values as a function of the error microphone position for: a) $\mu = 10^{-6}$ and b) $\mu = 1.2*10^{-4}$

Influence of the error microphone velocity

Fig. 7 shows also the influence of the error microphone velocity on the obtained disturbance attenuation. Maximum (and average as well) of the obtained attenuation decreases along with the increase of the error microphone velocity. The same conclusions give the analysis of the attenuation plots shown in Fig. 8. The time plots of attenuation $J(i)$ as a function of the error microphone position are shown for different values of v and μ. For very slow adaptation ($\mu = 10^{-6}$) the movement of the error microphone has only a slight influence on the obtained attenuation (Fig. 8a). While the performance of the ANC system with fast adaptation ($\mu = 1.2*10^{-4}$) is far better – the obtained attenuation is very high – it is also more significantly influenced by the fast movement of the error microphone (Fig. 8b).

SUMMARY

The ANC system creating 3-dimensional zones of quiet in the enclosure with the moving error microphone has been presented. It has been shown that in some conditions the standard FX-LMS algorithm can deal with the severe nonstationarities – the zone of quiet can adaptively track the movement of the error microphone. The behaviour of the ANC system has been illustrated by the results of real-world experiments. It has been shown that the larger value of the adaptation parameter of the adaptive control algorithm, the higher is the obtained attenuation. The given examples confirmed that the increasing intensity of the movement deteriorates the ANC system performance expressed by the disturbance attenuation. However, even for the velocity as high as 7 m/s the zone of quiet can track the error microphone.

The presented results of the preliminary experiments showed how powerful the adaptation can be if properly applied for fast-varying ANC systems. The research will be continued for more complicated disturbances and for other adaptive control algorithms.

REFERENCES

[1] Błażej M., Ogonowski Z., „Non-stationarity of 3-D Zones of Quiet” (in Polish), XLVIII *Otwarte Seminarium Akustyki OSA 2001*, 197-202, (2001)

[2] Elliott S.J., *Signal Processing for Active Control*, (Academic Press 2001)

[3] Kuo S.M., Morgan D.R, *Active Noise Control System. Algorithms and DSP Implementations*, (J. Wiley & Sons Inc., New York 1996)

[4] Michalczyk M.I., *Adaptive control algorithms for three-dimensional zones of quiet*. (Skalmierski Computer Studio, Gliwice, 2004)

[5] Michalczyk M.I. „Adaptive control algorithms for three-dimensional zones of quiet”, Archives of Control Sciences, **15(1)**, 53-82 (2005)

Acknowledgements

The partial financial support of the research of the Ministry of Education and Science under the grant 3 T11A 012 29 is gratefully acknowledged. The authors are indebted to prof. Z. Ogonowski for his contribution to concept, design and construction of the laboratory stand.